Molecular Wires

DOI: 10.1002/ange.201104700

Completely Encapsulated Oligothiophenes: Synthesis, Properties, and Single-Molecule Conductance**

Yutaka Ie, Masaru Endou, See Kei Lee, Ryo Yamada, Hirokazu Tada, and Yoshio Aso**

Since the concept of single molecular electronics has emerged as a complement to silicon-based electronics in terms of the bottom-up approach and ultimate miniaturization,[1,2] molecules for building components have been widely developed.[3–7] π-Conjugated molecules have attracted significant attention as molecular wires in molecular devices, and their potential has been shown by systematic studies of photo-induced charge transfer through their conjugated backbones.[8] Among the variety of π-conjugated systems reported thus far, structurally well-defined oligothiophenes have become one of the most actively investigated molecules for two reasons:[7] 1) oligothiophenes exhibit the longest effective conjugation length of known organic oligomers;[9] and 2) the high polarizability of the sulfur atom in thiophene effectively stabilizes the cationic species in various oxidation states. We previously reported the synthesis of a thiophene 24-mer bearing anchor groups at both terminal positions,[10] and we demonstrated the electrical conductance of the thiol-terminated oligothiophene with 10-nm-scale nanogap electrodes.[11] However, this measurement has remained ambiguous for precise single-molecule conductivity owing to the possibility of plural molecular connections between the electrodes and the possible π–π interactions between the molecules. A break junction (BJ) method involving the use of a scanning tunneling microscope (STM) has been established as a reliable technique for single-molecule measurement.[3] However, Mayor, Calame et al. recently reported that the intermolecular π–π interactions between adjacent molecules also contribute to form molecular bridges between metal electrodes in STM-based measurements.[12] To address this situation, we have focused on the encapsulation of the π-conjugated backbones to prevent intermolecular electronic communication (cross-talk).[13–15] Although the introduction of covalently bonded bulky substituents was expected to be a reliable encapsulation method, the molecular design of oligothiophenes that circumvents intermolecular interactions and yet maintains effective conjugation has proven to be difficult.[16] In particular, a compound incorporating bulky substituents at all repeating units, a so-called "defect-free molecule", that meets these criteria was only recently successfully synthesized.[17–20] We have succeeded in the creation of completely encapsulated oligothiophenes, *n*T′.[21] However, the steric bulk of the Si*t*BuPh$_2$ (TBDPS) groups in *n*T′ restricted the introduction of anchoring functional groups at the terminal α positions of the oligothiophenes, thus preventing conductivity measurements. Therefore, we predicted that a planar fluorene unit in place of the TBDPS groups would enhance the reactivity at the α positions. Thus, we have developed the appropriate π-conjugated systems *n*T ($n = 2$, 4, 6) and HSPh-*n*T-PhSH (introduction of anchor groups; $n = 2$, 4, 6) for the measurement of single-molecule conductivity (Figure 1). Although the conductance measurements[22,23] and conductance mechanism[24] of heterogeneously substituted oligothiophenes have been reported, the single-molecule conductivity measurement of homogeneously substituted oligothiophenes with both effective conjugation and complete encapsulation has never been achieved. Herein, we report the synthesis, structure, properties, and single-molecule conductivity of encapsulated oligothiophenes.

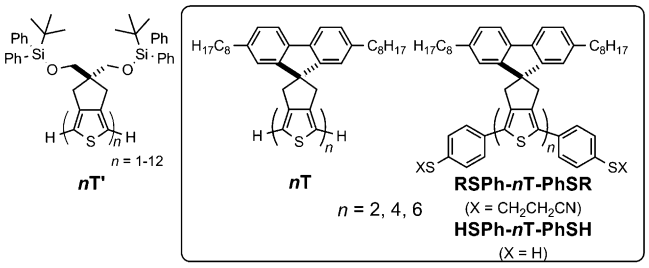

Figure 1. Chemical structures of encapsulated thiophene-based π-conjugated systems.

We envisioned that the zirconocene-mediated transformation of a diyne into a thiophene ring[25] was appropriate for the synthesis of our newly designed repeating unit. As shown in Scheme 1, the reaction of diyne **1**[26] with Negishi's reagent, generated in situ from [Cp_2ZrCl_2] and 2.0 equivalents of *n*BuLi, and subsequent treatment with S_2Cl_2 afforded **2** in a 79% yield. The direct bromination of **2** with NBS led to the formation of dibromothiophene **3**.

[*] Prof. Y. Ie, M. Endou, Prof. Y. Aso
The Institute of Scientific and Industrial Research (ISIR)
Osaka University
8-1 Mihogaoka, Ibaraki, Osaka 567-0047 (Japan)
E-mail: aso@sanken.osaka-u.ac.jp
Prof. Y. Ie
PREST-JST
4-1-8 Honcho, Kawaguchi, Saitama 333-0012 (Japan)
S. K. Lee, Prof. R. Yamada, Prof. H. Tada
Graduate School of Engineering Science, Osaka University
1-3 Machikaneyama, Toyonaka, Osaka 560-8531 (Japan)

[**] This work was supported by a Grant-in-Aid for Scientific Research from the Ministry of Education, Culture, Sports, Science and Technology (Japan), and the Management Expenses Grants for National Universities Corporations from the Ministry of Education, Culture, Sports, Science, and Technology (Japan). Thanks are given to the Comprehensive Analysis Center (CAC), ISIR, Osaka University, for assistance in obtaining elemental analyses.

Supporting information for this article is available on the WWW under http://dx.doi.org/10.1002/anie.201104700.

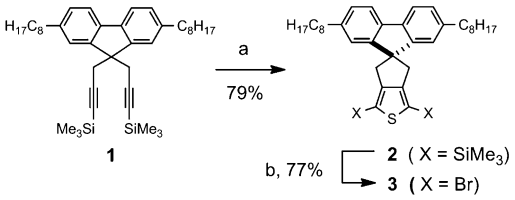

Scheme 1. Synthesis of monomer **3**. Reagents and conditions: a) 1) $[Cp_2ZrCl_2]$, *n*BuLi, THF, −78 °C 2) S_2Cl_2; b) NBS, DMF/$CHCl_3$ (1:1) 0 °C. DMF = *N*,*N*′-dimethylformamide, NBS = *N*-bromosuccinimide, THF = tetrahydrofuran.

Having the key monomer unit **3** in hand, we synthesized *n*T by using transition-metal-catalyzed aryl coupling reactions as summarized in Scheme S1 in the Supporting Information. The synthesis of HSPh-*n*T-PhSH is summarized in Scheme 2. The protected thiol group was successfully introduced to the stannylated bithiophene **4** by molar-ratio-controlled Stille coupling reactions with 4-(2-cyanoethylthio)bromobenzene (**5**) to give either RSPh-2T-PhSR or **6**. Subsequent palladium-catalyzed homocoupling of **6** in the presence of $CuCl_2$ afforded RSPh-4T-PhSR. The sexithiophene RSPh-6T-PhSR was obtained by the Stille coupling of **6** with **7**. Finally, the 2-cyanoethyl protecting groups in RSPh-*n*T-PhSR were easily removed by treatment with excess amounts of cesium hydroxide monohydrate to give HSPh-*n*T-PhSH. To prevent the formation of insoluble polymeric materials caused by disulfide formations, HSPh-*n*T-PhSH was kept in diluted mesitylene solutions after characterization by mass spectroscopy.

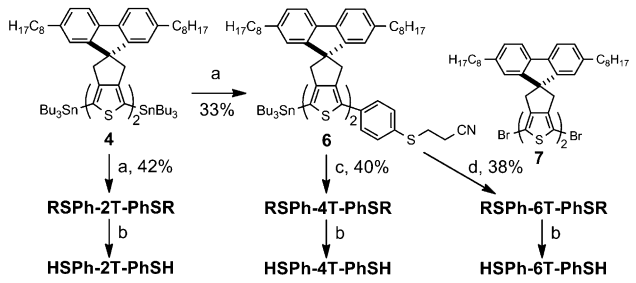

Scheme 2. Synthesis of HSPh-*n*T-PhSH. Reagents and conditions: a) $[Pd(PPh_3)_4]$, **5**, toluene, reflux; b) CsOH, *o*-dichlorobenzene/EtOH (4:1), 50 °C; c) $Pd(OAc)_2$, $CuCl_2$, THF, RT; d) $[Pd(PPh_3)_4]$, **7**, toluene, reflux.

To investigate the influence of the octyl-substituted fluorene unit, the crystal structure of 2T was determined by single-crystal X-ray diffraction analysis. Single crystals suitable for the analysis were obtained by slow evaporation from a *n*-hexane solution.[27] As shown in Figure 2, the molecule lies on a crystallographic center of symmetry, and thus, the neighboring thiophene rings adopt a *trans* conformation and a completely coplanar structure. The fluorene moieties are at a dihedral angle of 91.2° with respect to bithiophene, thus indicating orthogonal arrangement through the spiro carbon atom. As we expected, the octyl groups cover the conjugated backbone of the bithiophene without shielding the reactive terminal α position, thus yielding oligomers that feature suppressed intermolecular π–π interactions as well as maintain terminal functionalization versatility, as demonstrated by the oligomer synthesis.

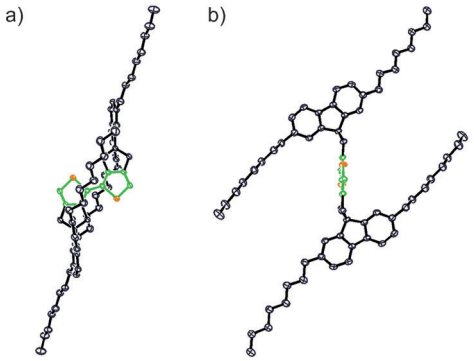

Figure 2. Crystal structure of 2T; a) top view and b) side view. Hydrogen atoms were omitted for clarity. Thermal ellipsoids drawn at 50% probability.

The electronic absorption spectra of *n*T and RSPh-*n*T-PhSR were measured in CH_2Cl_2 solutions; their absorption maxima are summarized in Table 1. These spectra show an absorption band in the visible region corresponding to the π–π* transition of the oligothiophene backbones as well as the π–π* transition of the fluorene unit centered at $\lambda = 280$ nm, as shown in Figure 3a. The absorption maxima derived from the transitions of the oligothiophene backbones shift to a longer wavelength when the number of thiophene rings increases from two to six. The absorption maxima of RSPh-*n*T-PhSR corresponding to the π–π* transition of conjugated backbones are red-shifted compared to the corresponding *n*T compounds (Figure 3b). This shift is due to the extension of the conjugation into the phenyl rings. The π–π* transition energies (E_T) of *n*T, *n*T′, and nonsubstituted oligothiophenes are plotted against the inverse of the number of thiophene rings ($1/n$) in Figure 3c. The linear relationship of the transition energy for *n*T is calculated to be E_T (eV) = 2.03 + 3.85/*n*. Its slope (3.85) is almost identical to that of *n*T′ (3.86),[21] and slightly steeper than that of nonsubstituted oligothiophenes (3.76).[28] This result clearly indicates that the presence of insulating fluorene units has little effect on the effective conjugation length.

The electrochemical properties of *n*T and RSPh-*n*T-PhSR were studied by cyclic voltammetry (CV) in $CHCl_3/CH_3CN$

Table 1: Photophysical and electrochemical properties.

Compounds	λ_{max} [nm][a]	E_T [eV][b]	$E_{p.a.}$ [V][c]
2T	314	3.95	+1.02[d]
4T	413	3.00	+0.37, +0.86[d]
6T	466	2.66	+0.21, +0.49
RSPh-2T-PhSR	399	3.11	+0.53
RSPh-4T-PhSR	457	2.71	+0.29, +0.55
RSPh-6T-PhSR	488	2.54	+0.11, +0.37

[a] In CH_2Cl_2. [b] $E_T = 1240/\lambda_{max}$. [c] In $CHCl_3/CH_3CN$ (10:1) containing 0.1 M $TBAPF_6$. V vs. Fc/Fc^+. [d] Irreversible.

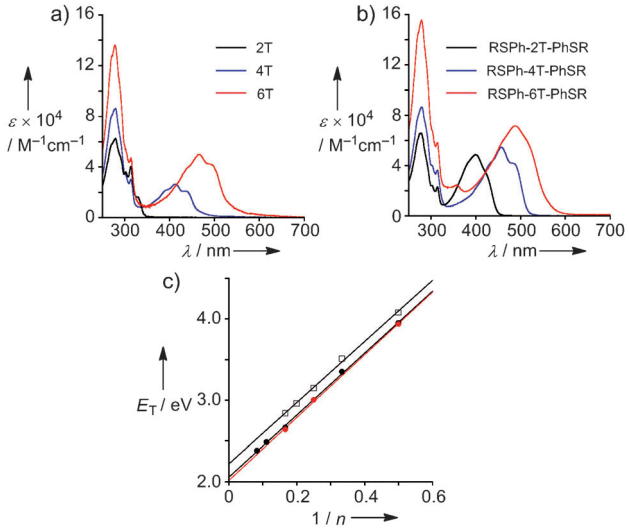

Figure 3. UV/vis absorption spectra of a) *n*T and b) RSPh-*n*T-PhSR in CH_2Cl_2. c) Correlations between transition energies (E_T) and the inverse of the number of thiophene rings ($1/n$) of nonsubstituted oligothiophenes (squares), *n*T′ (black circles), and *n*T (red circles).

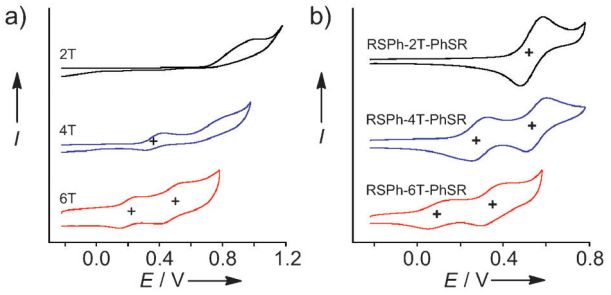

Figure 4. Cyclic voltammograms of a) *n*T and b) RSPh-*n*T-PhSR in $CHCl_3/CH_3CN$ (10:1) containing 0.1 M $TBAPF_6$.

(10:1) solutions containing 0.1 M tetrabutylammonium hexafluorophosphate ($TBAPF_6$), and the potentials are calibrated to ferrocene/ferrocenium (Fc/Fc^+). The cyclic voltammograms are shown in Figure 4a, and the oxidation potentials are listed in Table 1. An irreversible oxidation wave for 2T and reversible oxidation waves for 4T and 6T were observed. Note that all the oxidation waves are assigned to a one-electron oxidation process. The first oxidation potentials decrease with an increase in the conjugation length, which is in good agreement with our previously reported *n*T′ trend.[21] As shown in Figure 4b, reversible oxidations are observed for all of the thiol-protected compounds since the phenyl capping of the conjugated backbone increases the stability of the radical cationic species.

It is important to investigate the oxidized species of the synthesized oligothiophenes since the oxidized state of conjugated wire molecules is directly associated with the active carrier species in single-molecule conduction. Furthermore, positively charged oligothiophenes tend to spontaneously form intermolecular dimers (denoted as π dimers),[29] which we can exploit to evaluate the effect of encapsulation upon suppressing intermolecular interactions. Thus we measured the UV/Vis/NIR spectra of 6T as it was progressively oxidized with $SbCl_5$ at room temperature in CH_2Cl_2 and compared it with the behavior of the un-encapsulated dihexylsexithiophene Hex-6T. As shown in Figure 5a, upon one-electron oxidation of 6T, the band corresponding to the neutral π–π* transition centered at 2.7 eV was replaced by two bands assigned to the polaron (radical cation) at 0.8 and 1.6 eV. Furthermore, one-electron oxidation completely converted the polaron into a bipolaronic species (dication), which exhibited a new band at 1.2 eV. This behavior is in good agreement with the two one-electron oxidation waves observed in the CV. Similar spectral changes were also observed for Hex-6T (Figure 5b), thus showing that the conjugated backbones of these sexithiophenes are identical in unimolecular electronic properties. Note that these oxidized species are cleanly reduced to the neutral species by treatment with hydrazine. As mentioned above, it has been proposed that the polaronic species of oligothiophenes form π dimers between charged backbones. In fact, as shown in Figure 5d, when the polaronic species of Hex-6T was cooled to 223 K, new bands at 1.1 and 1.8 eV increased in intensity with a concomitant decrease in the intensity of the polaronic bands, which is an evidence of π-dimer formation. In contrast, the polaronic species of 6T, upon cooling to 223 K, did not exhibit such spectral band transposition to a higher energy (Figure 5c). This significant difference between the behavior of 6T and Hex-6T can clearly be explained by the encapsulation effect on suppressing the π-dimer formation of the 6T polaron and thus insulating the π-conjugated backbones.

Electrical conductance of the molecules was measured using the BJ method by STM.[3] The STM/BJ measurement was carried out using mechanically cut gold tips in a 0.1 μM (approximate) mesitylene solution of the molecules at room temperature. The substrate was epitaxially grown Au(111) on mica. Procedures for BJ measurements have been described previously.[23] The conductance of the metal/molecule/metal (MMM) junctions is determined from a conductance histogram created from 500–1000 measurements. Figure 6a shows

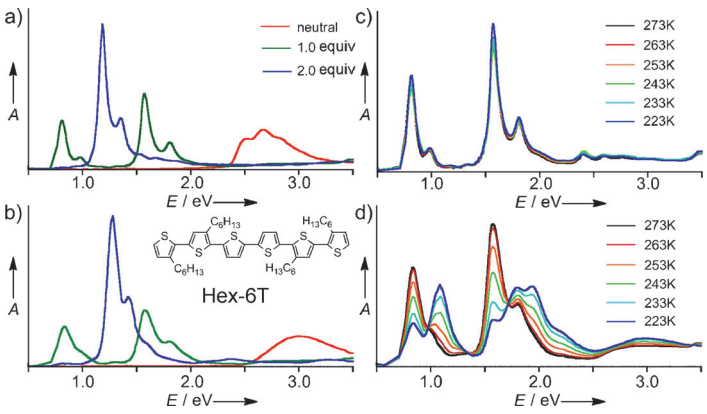

Figure 5. UV/Vis/NIR spectra of a) 6T and b) Hex-6T in CH_2Cl_2 under oxidation with $SbCl_5$. Variable temperature UV/Vis/NIR spectra of c) polaronic species 6T and d) polaronic species Hex-6T in CH_2Cl_2.

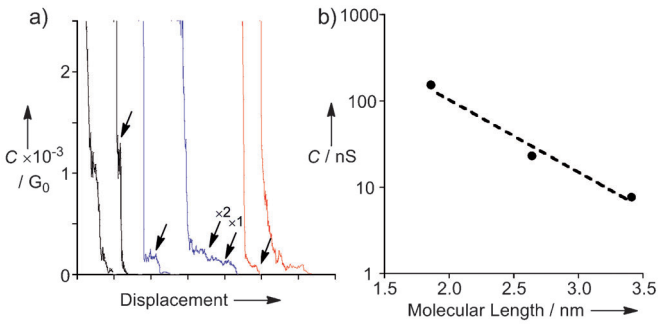

Figure 6. a) Conductance transient curves of HSPh-2T-PhSH (black), HSPh-4T-PhSH (blue), and HSPh-6T-PhSH (red). Plateaus are indicated by the arrows. Example of the conductance transient curve showing multiple plateaus is shown in HSPh-4T-PhSH. b) Conductance of HSPh-*n*T-PhSH as a function of molecular length.

a typical conductance transient curves obtained during the retraction of the STM tip after contact with the substrate in the solution of HSPh-*n*T-PhSH. Plateaus that were observed at values smaller than G_0 were attributed to the conductance of the MMM junctions since no plateaus were observed in the same conductance region in pure mesitylene. Several plateaus were sometimes observed in sequence as indicated by the arrows in the transient curve of HSPh-4T-PhSH. The sequential plateau appeared at the conductance of integer multiples of the smallest plateau, thus, were attributed to the decrease of the number of molecules bridging the substrate and the STM tip in parallel. On the basis of the features observed in current transient curves, we concluded that MMM junctions were formed by HSPh-*n*T-PhSH. The conductance of the MMM junctions were determined from the conductance histogram as shown in Figure S1 (see the Supporting Information). The solid arrows in Figure S1 indicate the peak positions attributed to the single-molecule conductance. Figure 6b shows a semilog plot of the conductance as a function of the molecular length. The tunneling transport was evident from the exponential decrease in the conductance with molecular length, which is expressed as $G\exp(-\beta n)$ where β is a decay constant, and n is the number of thiophene rings or the length of the conduction channel. The decay constant of the present encapsulated oligothiophene was estimated to be $\beta = 1.9\ \mathrm{nm}^{-1}$ from the observed values shown in Figure 6b. This value is in agreement with that obtained from theoretical calculations for nonsubstituted oligothiophenes ($\beta = 2.11\ \mathrm{nm}^{-1}$).[30] According to density functional theory (DFT) calculations at the B3LYP/6-31 G(d, p) level of theory, the distribution and energy level of the HOMO of 6T is almost identical to that of the nonsubstituted thiophene 6-mer (see Figure S2 in the Supporting Information). These results indicate that the molecules synthesized in the present study possess the intrinsic electronic structures and transport properties of defect-free oligothiophenes with effective conjugation.

In summary, a series of oligothiophenes whose structures were orthogonally fused with octyl-substituted fluorene were designed and successfully synthesized. The fluorene units play an important role as sterically compact encapsulating units, which enabled us to introduce anchoring functional groups at the terminal positions in the conjugated backbones. The complete encapsulation of the conjugated backbone and the high co-planarity of the thiophene rings of 2T were unambiguously revealed by the X-ray crystallographic analysis. The UV/vis absorption and CV measurements indicated that effective conjugation is maintained in the full oligomer series. The UV/Vis/NIR measurements of the oxidized species revealed the absence of intermolecular interactions between the conjugated backbones. The measurement of the single-molecule conductance was successfully carried out using modified STM techniques, and the decay constant β was estimated to be $1.9\ \mathrm{nm}^{-1}$. To our knowledge, this is the first experimentally determined β value of oligothiophenes composed by an electronically equivalent repeating unit. Furthermore, since we have obtained this result by the use of highly planar oligothiophenes in the absence of intermolecular interactions, this value could become a standard for forthcoming π-conjugated systems. Therefore, we conclude that our newly developed encapsulated oligothiophenes have enabled the elucidation of the electrical characterization of molecular wires. Additional investigations to increase the molecular length as well as to introduce optimized anchoring units to make encapsulated oligothiophenes applicable as single-molecule devices are currently underway in our group.

Received: July 7, 2011
Published online: September 14, 2011

Keywords: conducting materials · conjugation · cyclic voltammetry · single-molecule studies · synthetic methods

[1] A. Aviram, M. A. Ratner, *Chem. Phys. Lett.* **1974**, *29*, 277–283.
[2] a) N. J. Tao, *Nat. Nanotechnol.* **2006**, *1*, 173–181; b) J. C. Cuevas, E. Scheer, *Molecular Electronics: An Introduction to Theory and Experiment*, World Scientific, Singapore, **2010**.
[3] B. Xu, N. J. Tao, *Science* **2003**, *301*, 1221–1223.
[4] a) J. K. Whitesell, H. K. Chang, *Science* **1993**, *261*, 73–76; b) Y. Ie, T. Hirose, H. Nakamura, M. Kiguchi, N. Takagi, M. Kawai, Y. Aso, *J. Am. Chem. Soc.* **2011**, *133*, 3014–3022.
[5] K. Matsuda, H. Yamaguchi, T. Sakano, M. Ikeda, N. Tanifuji, M. Irie, *J. Phys. Chem. C* **2008**, *112*, 17005–17010.
[6] a) J. Roncali, *Chem. Rev.* **1997**, *97*, 173–205; b) J. Gierschner, J. Cornil, H.-J. Egelhaaf, *Adv. Mater.* **2007**, *19*, 173–191.
[7] a) A. Mishra, C.-Q. Ma, P. Bäuerle, *Chem. Rev.* **2009**, *109*, 1141–1276; b) I. F. Perepichka, D. F. Perepichka, *Handbook of Thiophene-based Materials*, Wiley-VCH, Weinheim, **2009**; c) L. Luo, S. H. Choi, C. D. Frisbie, *Chem. Mater.* **2011**, *23*, 631–645.
[8] T. Nakamura, M. Fujitsuka, Y. Araki, O. Ito, J. Ikemoto, K. Takimiya, Y. Aso, T. Otsubo, *J. Phys. Chem. B* **2004**, *108*, 10700–10710.
[9] T. Izumi, S. Kobashi, K. Takimiya, Y. Aso, T. Otsubo, *J. Am. Chem. Soc.* **2003**, *125*, 5286–5287.
[10] M. Endou, Y. Ie, T. Kaneda, Y. Aso, *J. Org. Chem.* **2007**, *72*, 2659–2661.
[11] N. Hatanaka, M. Endo, S. Okumura, Y. Ie, R. Yamada, Y. Aso, K. Tanaka, H. Tada, *Chem. Lett.* **2007**, *36*, 224–225.
[12] S. Wu, M. T. González, R. Huber, S. Grunder, M. Mayor, C. Schönenberger, M. Calame, *Nat. Nanotechnol.* **2008**, *3*, 569–574.
[13] M. J. Frampton, H. L. Anderson, *Angew. Chem.* **2007**, *119*, 1046–1083; *Angew. Chem. Int. Ed.* **2007**, *46*, 1028–1064.
[14] G. Wenz, B.-H. Han, A. Müller, *Chem. Rev.* **2006**, *106*, 782–817.

[15] J. Terao, S. Tsuda, Y. Tanaka, K. Okoshi, T. Fujihara, Y. Tsuji, N. Kambe, *J. Am. Chem. Soc.* **2009**, *131*, 16004 – 16005.
[16] W.-S. Li, D.-L. Jiang, T. Aida, *Angew. Chem.* **2004**, *116*, 3003 – 3007; *Angew. Chem. Int. Ed.* **2004**, *43*, 2943 – 2947.
[17] S. Tanaka, Y. Yamashita, *Synth. Met.* **2001**, *119*, 67 – 68.
[18] a) A. Wakamiya, D. Yamazaki, T. Nishinaga, T. Kitagawa, K. Komatsu, *J. Org. Chem.* **2003**, *68*, 8305 – 8314; b) T. Nishinaga, A. Wakamiya, D. Yamazaki, K. Komatsu, *J. Am. Chem. Soc.* **2004**, *126*, 3163 – 3174.
[19] D. Lee, T. M. Swager, *J. Am. Chem. Soc.* **2003**, *125*, 6870 – 6871.
[20] K. Sugiyasu, Y. Honsho, R. M. Harrison, A. Sato, T. Yasuda, S. Seki, M. Takeuchi, *J. Am. Chem. Soc.* **2010**, *132*, 14754 – 14756.
[21] Y. Ie, A. Han, T. Otsubo, Y. Aso, *Chem. Commun.* **2009**, 3020 – 3022.
[22] a) B. Q. Xu, X. L. Li, X. Y. Xiao, H. Sakaguchi, N. J. Tao, *Nano Lett.* **2005**, *5*, 1491 – 1495; b) S. Yasuda, S. Yoshida, J. Sasaki, Y. Okutsu, T. Nakamura, A. Taninaka, O. Takeuchi, H. Shigekawa, *J. Am. Chem. Soc.* **2006**, *128*, 7746 – 7747.
[23] R. Yamada, H. Kumazawa, T. Nobutoshi, S. Tanaka, H. Tada, *Nano Lett.* **2008**, *8*, 1237 – 1240.
[24] R. Yamada, H. Kumazawa, S. Tanaka, H. Tada, *Appl. Phys. Express* **2009**, *2*, 025002.
[25] P. J. Fagan, W. A. Nugent, *J. Am. Chem. Soc.* **1988**, *110*, 2310 – 2312.
[26] The synthesis of **1** is described in the Supporting Information.
[27] CCDC 832484 (2T) contains the supplementary crystallographic data for this paper. These data can be obtained free of charge from The Cambridge Crystallographic Data Centre via www.ccdc.cam.ac.uk/data_request/cif.
[28] G. Bidan, A. De Nicola, V. Enée, S. Guillerez, *Chem. Mater.* **1998**, *10*, 1052 – 1058.
[29] a) T. Sakai, T. Satou, T. Kaikawa, K. Takimiya, T. Otsubo, Y. Aso, *J. Am. Chem. Soc.* **2005**, *127*, 8082 – 8089; b) K. M. Knoblock, C. J. Silvestri, D. M. Collard, *J. Am. Chem. Soc.* **2006**, *128*, 13680 – 13681.
[30] G. Peng, M. Strange, K. S. Thygesen, M. Mavrikakis, *J. Phys. Chem. C* **2009**, *113*, 20967 – 20973.

